

Title:

Interaction of a Dimeric Single-Stranded DNA-Binding Protein (G5P) with DNA Hairpins. A Molecular Beacon Study

Author(s):

Tihomir Solomun, Leo Cordsmeier, Dorothea C. Hallier, Harald Seitz, and Marc Benjamin Hahn

Document type: Preprint

Terms of Use: Copyright applies. A non-exclusive, non-transferable and limited right to use is granted. This document is intended solely for personal, non-commercial use.

Citation:

"Tihomir Solomun u.a., J. Phys. Chem. B 2023, XX, XX, XXX-XXX ; <https://doi.org/10.1021/acs.jpcc.3c03669>"
Archiviert unter <http://dx.doi.org/10.17169/refubium-40583>

1
2
3
4
5
6
7
8
9
10
11
12
13
14
15
16
17
18
19
20
21
22
23
24
25
26
27
28
29
30
31
32
33
34
35
36
37
38
39
40
41
42
43
44
45
46
47
48
49
50
51
52
53
54
55
56
57
58
59
60

The Interaction of a Dimeric Single-Stranded DNA-Binding Protein (G5P) with DNA Hairpins. A Molecular Beacon Study

Tihomir Solomun,^{*,†} Leo Cordsmeier,^{†,‡} Dorothea C. Hallier,^{†,¶,§} Harald Seitz,^{¶,§}
and Marc Benjamin Hahn^{*,†}

[†]*Bundesanstalt für Materialforschung und -prüfung (BAM), 12205 Berlin, Germany*

[‡]*Freie Universität Berlin, Institut für Chemie, 14195 Berlin, Germany*

[¶]*Universität Potsdam, Institut für Biochemie und Biologie, 14476 Potsdam, Germany*

[§]*Fraunhofer Institut für Zelltherapie und Immunologie Institutsteil Bioanalytik und
Bioprozesse IZI-BB, 14476 Potsdam, Germany*

Abstract

Gene-V Protein (G5P/GVP) is a single-stranded (ss)DNA-binding protein (SBP) of bacteriophage ϕ 1 that is required for DNA synthesis and repair. In solution it exists as a dimer that binds two antiparallel ssDNA strands with high affinity in a cooperative manner, forming a left-handed helical protein-DNA filament. Here we report on fluorescence studies of the interaction of G5P with different DNA oligonucleotides having a hairpin structure (molecular beacon, MB) with a seven base-pair stem (dT24-stem7, dT18-stem7), as well as with DNA oligonucleotides (dT38, dT24) without a defined secondary structure. All oligonucleotide were end-labeled with a Cy3-fluorophore and a BHQ2-quencher. In the case of DNA oligonucleotides without a secondary structure, an almost complete quenching of their strong fluorescence (with about 5 % residual intensity) was observed upon the binding of G5P. This implies an exact alignment of ends of the DNA strand(s) in the saturated complex. The interaction of the DNA hairpins with G5P lead to the unzipping of the base-paired stem as revealed by fluorescence measurements, fluorescence microfluidic mixing experiments and electrophoretic mobility shift assay (EMSA) data. Importantly, the disruption of ssDNAs secondary structure agrees with the behavior of other single-stranded DNA-binding proteins (SBPs). In addition, substantial protein-induced fluorescence enhancement (PIFE) of the Cy3-fluorescence was observed.

Introduction

Single-stranded DNA-binding proteins (SBP) are essential for DNA replication, recombination, and repair in all known organisms.¹ Although their primary function is to provide protection for transiently formed single-stranded DNA (ssDNA),² SBP-ssDNA complexes additionally play highly dynamic functional roles,³ for example in disrupting ssDNA secondary structures.^{4,5} One such structure is a so called hairpin structure, a key building block not only of DNA but of many folded secondary structures found in nature, such as ribozymes, miRNA, shRNA and mRNA. A hairpin consists of a base paired double-stranded DNA part

1
2
3 (stem) and a loop sequence with unpaired nucleotides. When used as a sensing system like
4 in the presented study, hairpin structures are usually labeled with photoluminescent species
5 (one donor and one acceptor) at their two ends. Such labeled hairpin structures are called
6 molecular beacons (MB). The stem part of a MB brings the donor dye and the acceptor dye
7 (fluorescence quencher in this case) in proximity and ensures efficient quenching of the flu-
8 orescence emission, as well as signal generation when structural changes occur. This is why
9 the MB technique is a powerful analytical tool that, among other applications, can provide
10 information on SBP-DNA interactions.⁵⁻⁸ Fluorescence methods in general have proven to
11 be extremely useful for quantitative studies of the equilibria and kinetics of protein-DNA
12 interactions.⁹

13
14
15 In this study, we investigate the interactions of Gene-V Protein (G5P) and several ssDNA
16 MBs, with and without a secondary structure. G5P is a single-stranded DNA-binding protein
17 (SBP) of bacteriophage ϕ 1 that is required for DNA synthesis and repair. G5P was chosen
18 since it is a well-studied SBP prototype. Its properties, structure, and complex formation
19 with ssDNA was previously examined by electron microscopy,¹⁰ circular dichroism,¹¹ surface
20 plasmon resonance,^{12,13} Raman spectroscopy,¹³ fluorescence,¹² small-angle X-ray scattering
21 (SAXS),¹⁴ NMR¹⁵ and mass spectrometry¹⁶ methods. G5P also serves as a model system
22 in radiation research for investigations of the chemistry of DNA-protein crosslink forma-
23 tion, as can be found in cancerous tissue with high radiation resistance.^{14,17,18} The G5P
24 protein monomer has a molecular weight of 9.7 kDa and consists of 87 amino acids in a sin-
25 gle polypeptide chain which are mostly in the β -conformation, organized as a five-stranded
26 antiparallel β -sheet and two antiparallel β -ladder loops with a broad connecting loop.¹⁹ The
27 DNA binding motif is shared with the ssDNA-binding motif of human replication protein
28 A.²⁰ In solution G5P exists as a dimer with a 2-fold rotational symmetry axis and the DNA-
29 binding clefts positioned to bind two antiparallel ssDNA strands (Fig. 1).^{10,21} G5P, as well
30 as other single-stranded DNA-binding proteins, saturates ssDNA with a high cooperativity
31 of binding (cooperativity factor in the range of 500-5000).^{22,23} The number ($n = Nt/G5P$)
32
33
34
35
36
37
38
39
40
41
42
43
44
45
46
47
48
49
50
51
52
53
54
55
56
57
58
59
60

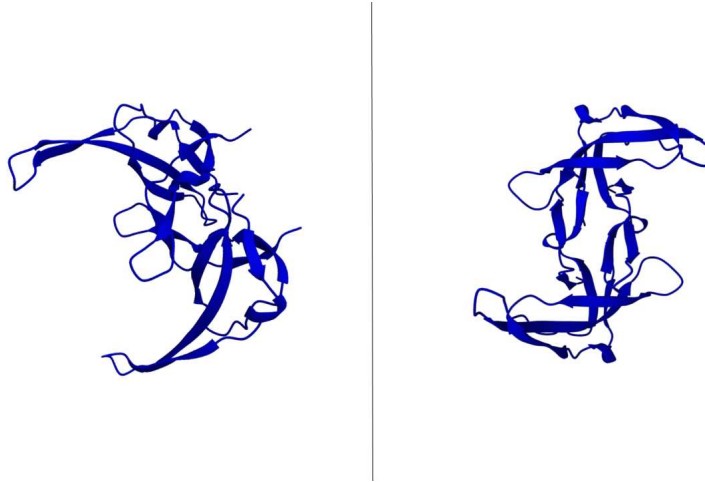


Figure 1: Schematic drawing of the G5P dimer from two different perspectives. The two ssDNA-binding clefts which enclose two ssDNA strands are evident. The DNA bases are embedded in G5P and the phosphate backbone of the two DNA strands points towards each other. G5P dimer image created from the PDB structure 1GVP.²¹

of nucleotides (Nt) bound per G5P monomer (G5P) depends on the binding conditions. The $n=4$ binding mode is dominant when the Nt to G5P ratio in solution is higher than 4.²⁴⁻²⁶ Below this ratio, the formation of more perfect G5P-ssDNA filaments and the occurrence of the $n=3$ binding-mode was reported.²⁴⁻²⁶ On the other hand, the G5P binding mode for dT oligonucleotides with more than 15 nucleotides was determined directly using ionization-mass spectrometry (ESI-MS) and, independently, size-exclusion chromatography to be predominantly $n=4$.¹⁶ The concentrations of G5P and oligonucleotides used there are comparable to this work. The accurate mass determination provides a precise measure of binding stoichiometry. We therefore assumed throughout the manuscript the G5P binding mode $n=4$. Furthermore, in complexes with phage DNA in vivo, G5P dimers form a superhelical structure.²⁷ Within the superhelix, each protein dimer is bound, with its two-fold symmetry, to the same strand of a long DNA going in opposite directions.¹⁹ Thus, the DNA must wrap back at the ends of the complex. Size-exclusion chromatography and mass spectrometry experiments established that the dT16 oligonucleotide forms 4:1 complexes with G5P, suggesting that the 16-mer is long enough to fold back and to interact with all the four DNA binding sites in the protein dimer of dimers.¹⁶ In addition, at least for the dT18

1
2
3 oligonucleotides, the mass-spectroscopy work cited above showed that in the concentration
4 ranges corresponding nominally from $n=6$ to $n=3$ the binding mode remains unchanged.¹⁶
5
6 The data presented in this work reveals a number of different processes and effects and pos-
7 sibly represents an important base for adequate interpretation of more sophisticated single-
8 molecule Förster resonance energy transfer (smFRET) investigations of the ssDNA-G5P
9 system in the future.
10
11
12
13
14
15
16

17 **Experimental**

18 **G5P expression and purification**

19
20
21 The Gene-V Protein (G5P/GVP, Swissprot: P69544, 87 AA, Mw 9688 Da) from bacterio-
22 phage f1 was expressed and purified as follows: The G5P plasmid pET-30b was transformed
23 into BL21:DE3 and grown on a 2YT agar plate with 50 $\mu\text{g}/\text{mL}$ kanamycin overnight. A
24 single colony was used for a 10 mL overnight culture in 2-YT medium. Two mL of overnight
25 culture was inoculated into 200 mL of 2YT medium with 50 $\mu\text{g}/\text{mL}$ kanamycin. The protein
26 was expressed with 1 mM IPTG (end concentration) after $\text{OD}_{600} = 0.5$ was reached for 4 h.
27 Cells were collected, resuspended in 5 mL of buffer ($1 \times \text{PBS}$, with 25 mM NaCl), and soni-
28 cated. Cell debris was removed, and the supernatant purified with a 1 mL Resource Q anion
29 exchange column using the ÄKTA FPLC (both GE Healthcare, Sweden). The flow through
30 was collected and purified using 1 mL of Ni-NTA agarose (Qiagen, Germany). Resin was
31 washed three times with 5 mL of buffer ($1 \times \text{PBS}$, 20 mM imidazole), and incubated for 30
32 min with the flow through of the Q anion exchange column and the protein eluded with 5 mL
33 of buffer ($1 \times \text{PBS}$, 250 mM imidazole). Eluate was concentrated in ultracentrifuge devices
34 to a final concentration of 1.5 mg/mL and the buffer was changed to $1 \times \text{PBS}$ using dialysis
35 tubes (both Merck Chemicals, Germany). The protein concentration was determined by
36 BCA assay. Protein was stored at $-20 \text{ }^\circ\text{C}$.
37
38
39
40
41
42
43
44
45
46
47
48
49
50
51
52
53
54
55
56
57
58
59
60

Oligonucleotides

The labeled oligonucleotides were obtained from Eurofins Genomics, Germany (HPLC purified and lyophilized). The abbreviations (Fig. 2), for example dT24stem7, stands for molecular beacons (MB) with dT24 loop and the stem of seven nucleotide pairs (Cy3-5'-GCTGACT-dT24-AGTCAGC-3'-BHQ2). The stem was identical in all cases.


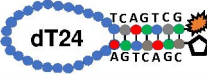
	Abbreviation			
	dT24	dT38	loop18stem7	loop24stem7
Structure	-	-	hairpin 	hairpin 
Sequence	Cy3-5'-dT24-3'-BHQ2	Cy3-5'-dT38-3'-BHQ2	Cy3-5'-GCTGACT-dT18-AGTCAGC-3'-BHQ2	Cy3-5'-GCTGACT-dT24-AGTCAGC-3'-BHQ2
Binding capacity of G5P dimers:				
n=4 mode	3	5	4 (loop: 2)	5 (loop: 3)
n=3 mode	4	6	5 (loop: 3)	6 (loop: 4)

Figure 2: Structures and abbreviations of the MBs in this work, as well as their binding capacity for G5P dimers in binding modes n=4 and n=3 ($n=Nt/G5P$). Star represents Cy3 and pentagon BHQ2 quencher.

Electrophoretic Mobility Shift Assay

Electrophoretic Mobility Shift Assay (EMSA) measurements were carried out using samples with 2.5 μ M loop18stem7 hairpin oligonucleotide mixed with different G5P concentrations (0 μ M, 17.5 μ M, 35 μ M and 75 μ M) in 1x PBS solution. A 2% agarose gel was cast using 0.5x TRIS-Borat-EDTA-buffer (TBE-buffer, Merck Chemicals Germany) as solvent. The oligonucleotide and increasing amounts of G5P were incubated for 20 min at 30 °C, and then applied to the gel. Gel was run for 60 min at 60 V. The Agarose Gel was scanned via an

Amersham Typhoon Biomolecular Imager (GE Healthcare, Sweden) with excitation over a broad range from 513 to 556 nm. The emission was detected between 570-613 nm according to the fluorescence properties of Cy3 fluorophore.

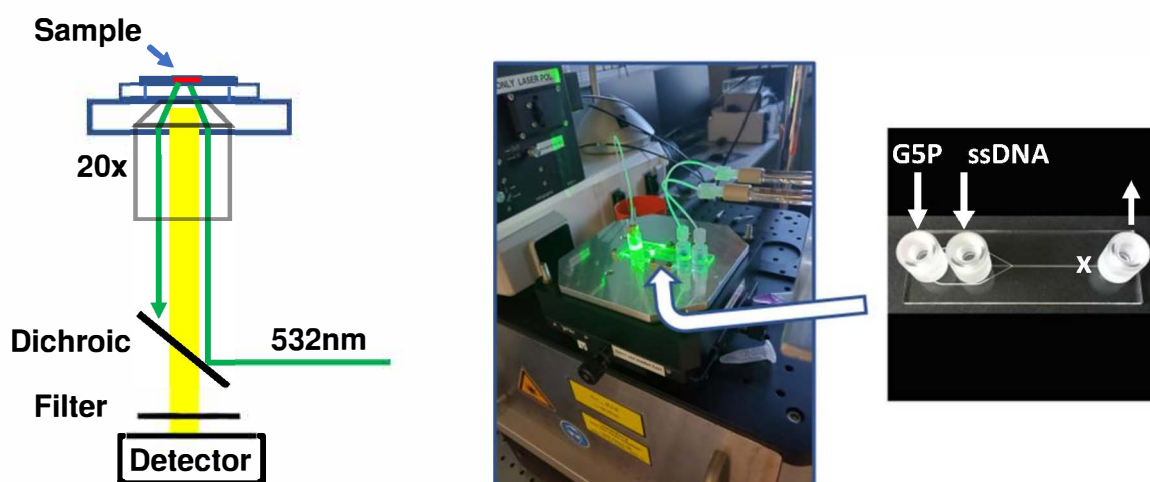


Figure 3: (Left) Schematic drawing of the experimental setup used for the Cy3-fluorescence observations. The 532 nm laser light was focused into a 15 μ l sample drop sitting on top of a cover slide or in the channel of the microfluidic mixing device. (Center) Photograph of the experimental setup for the dynamic fluorescence measurements and (Right) of the glass microfluidics herringbone mixing device (Darvin Microfluidics). G5P was injected into the mixing part of the device from the two outside channels and the DNA from the middle channel. The laser light coming from below was focused inside the channel close to the outlet (marked with x). During the measurements the mixer was shielded from the outside light (not shown).

Equilibrium fluorescence measurements

The measurements were carried out using a confocal Raman Microscope (Witec alpha300R) equipped with a 20x Zeiss EX Epiplan DIC objective (working distance 3 mm, numerical aperture 0.4), a laser (wavelength 532 nm), spectrometer UHTS-300-VIS (grid of 600 grat-

ings/mm) and a thermoelectrically cooled CCD-camera Andor DV-401A-BV-532 (at -62°C). The laser light was focused: a) into a 15 μl drop of solution on a high-precision cover glass slide (Zeiss, 18 mm x 18 mm x 0.18 mm) in a high-humidity atmosphere to avoid evaporation as described previously in detail,²⁸ or b) inside the microfluidic channel of the mixing device. Laser power (0.1 mW) was checked by Coherent Laser check device. For equilibrium measurements G5P-DNA solutions were mixed 30 min before the fluorescence measurements. Ten spectra were recorded with an integration time of 0.5 sec. The temperature during the measurement was $24\pm 2^{\circ}\text{C}$. All the resulting data are an average over an ensemble of molecules. Therefore, the registered fluorescence signal has to be interpreted as an ensemble average.

Time dependent measurements in the Herringbone Mixer

The Herringbone Mixer (Fig. 3) was obtained from Darwin (darwin-microfluidics.com). The microchannel of the mixer is structured with asymmetric herringbone-shaped grooves on its bottom to generate helical flow and chaotic stirring for mixing the two liquids injected in parallel. The two microfluidic entry channels serve to introduce ssDNA and G5P protein into the herringbone structured mixing part of the device. The laser light was focused directly into the channel close to the exit of the device. Protein and ssDNA were injected from two syringes within 2s while the fluorescence spectra were taken continuously over at least 150s at the focal spot.

Results and discussion

To provide comprehensive information about the G5P-DNA interaction, two oligonucleotides without a secondary structure, namely dT24 and dT38, were studied in comparison to two oligonucleotides with a hairpin structure, dT18stem7 and dT24stem7 (Fig. 4). We point out here, that the chosen DNA sequences do not naturally exist in bacteriophage $\phi 1$, and

1
2
3 their combination with G5P represent an optimized model system to obtain a mechanistic
4 understanding of protein-DNA interaction and protein induced fluorescence enhancement
5 (PIFE) phenomenon, aimed towards nanotechnology, sensing and controlled release, as well
6 as functionalization of (bio)polymers. The fluorescence spectra of the DNA without G5P
7 (red curves) and DNA+G5P (blue curves) in equilibrium and their intensities (at maximum
8 at 576 nm) are presented in Figs. 4 and 5, respectively. In the case of the pure oligonu-
9 cleotides without secondary structure (A and B in Fig. 4, red curves) the shorter oligonu-
10 cleotide demonstrates lower fluorescence intensity. This agrees with a smaller persistence
11 length between the fluorophore and the quencher for the shorter oligonucleotide as revealed
12 in a study probing single-stranded DNA conformational flexibility using single-molecule sm-
13 FRET.²⁹ Upon binding of G5P a nearly complete extinction of the Cy3 fluorescence (with
14 5% residual intensity) is observed for both oligonucleotides (Fig. 4 A and B, blue curves).
15 This is consistent with the known fundamental property of the G5P-ssDNA superhelix ge-
16 ometry and implies the alignment of the antiparallel ends of the DNA and proximity of Cy3
17 and BHQ2. It is interesting here to juxtapose this behavior with the behavior of the single-
18 stranded DNA-binding protein SSB. SSB binds to ssDNA, among other modes, by wrapping
19 65 DNA nucleotides around its tetramer. Only at this binding geometry are the two ends of
20 the ssDNA in proximity to each other.⁶

21
22
23
24
25
26
27
28
29
30
31
32
33
34
35
36
37
38
39 The spectra in C and D in Fig. 4 show the behaviors of two MB with hairpins and loops
40 of different lengths. The lower fluorescence intensity of the probe with the smaller loop (D)
41 agrees with an earlier study of the loop-size dependence of DNA and RNA hairpin stabil-
42 ity and their folding/unfolding kinetics using laser temperature-jump spectroscopy.³⁰ These
43 measurements revealed a steep dependence of single-stranded DNA hairpin stability on the
44 length of the loop (L). The folding times (t) for ssDNA hairpins increased with loop size as
45 $t \sim L^{2.2}$.³⁰ In contrast to the oligonucleotides without secondary structure (Fig. 4, A and B)
46 the MB with hairpins show an increase in the fluorescence upon binding of G5P (Fig. 4 C and
47 D, blue curves and Fig. 5 blue bars). This increase is dependent on the G5P concentration
48
49
50
51
52
53
54
55
56
57
58
59
60

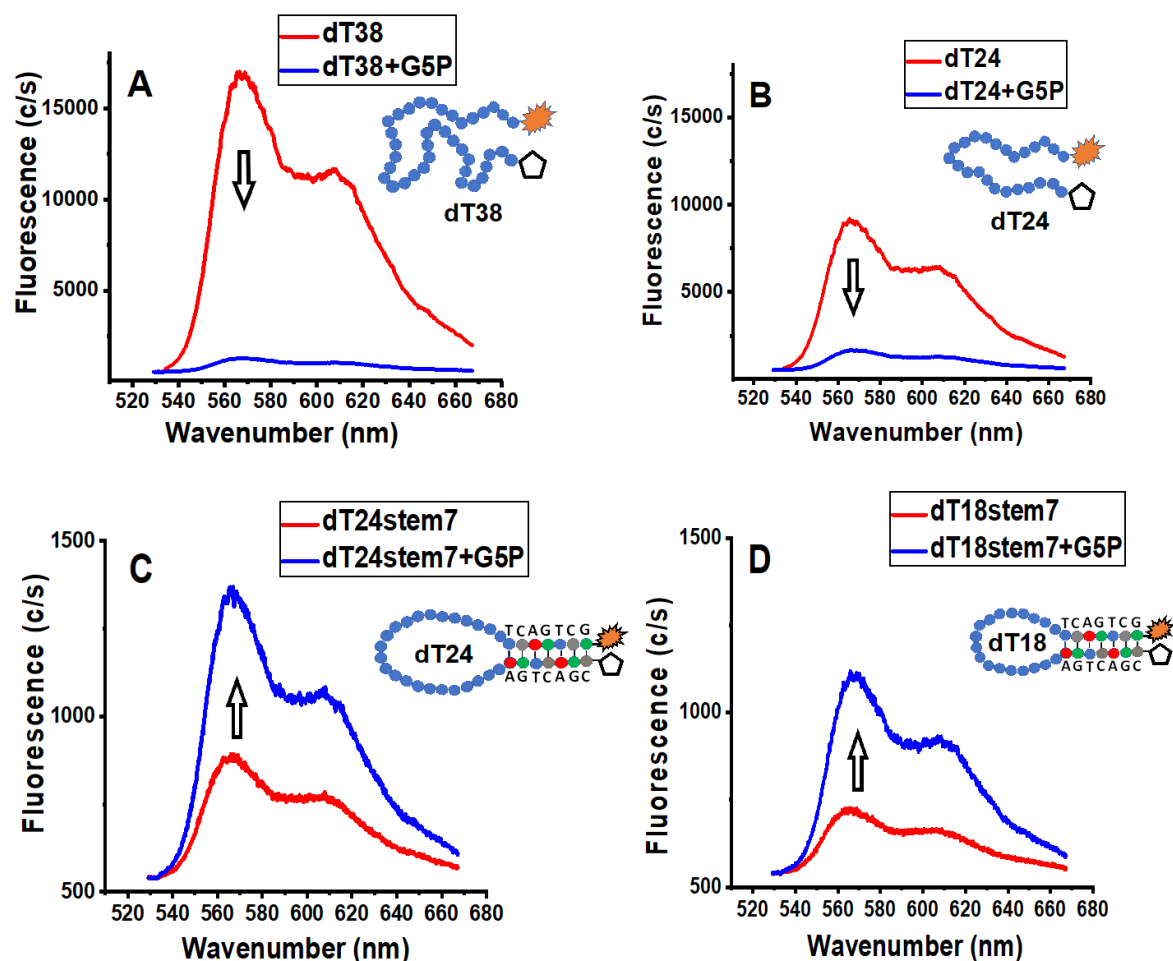


Figure 4: Cy3-fluorescence before and after binding of G5P protein. A) and B) oligonucleotides without secondary structure. C) and D) DNA hairpin probes. The star depicts Cy3 and the pentagon BHQ2. The notation shortcut, for example, dT24stem7 stands for MB with a dT24 loop and the stem of seven nucleotide pairs (Cy3-5'-GCTGACT-dT24-AGTCAGC-3'-BHQ2). The stem is the same in all cases. The concentration of all oligonucleotides and hairpins is 2.5 μ M and that of the G5P protein 75 μ M, with dilution due to the mixing already considered. Note the different Y scales between A, B and C, D, respectively. We point here that at these concentrations there is also contributions of PIFE effect to the spectra (see text).

and the Nt/G5P ratio in solution (see below). We point here nearly equal signal height in the presence of G5P for all constructs (Fig. 4 and 5).

In Fig.6 the dependence of the fluorescence intensity of two dT38 probes, one containing

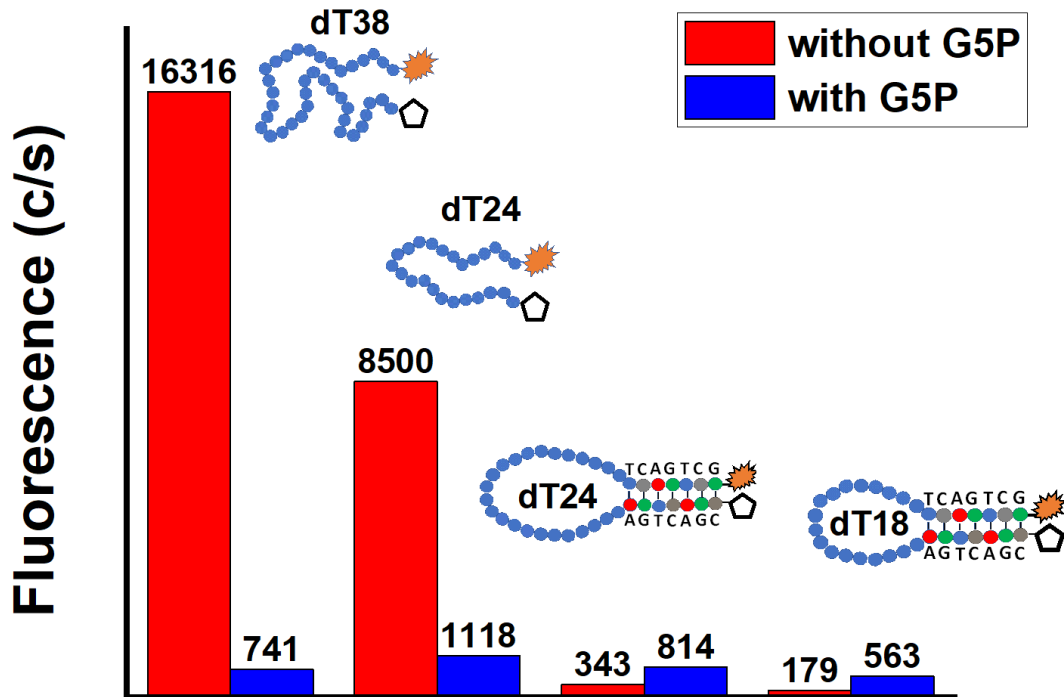


Figure 5: Fluorescence intensities at the maximum (567 nm) of the emission spectra in Fig. 4 after linear background subtraction.

only the Cy3 fluorophore (control oligonucleotide, upper graph) and the other having both Cy3 and BHQ2 quencher attached to it (lower graph), on the $n=Nt/G5P$ ratio and the G5P concentration is presented. At low G5P concentrations (high Nt/G5P ratio) the Cy3-dT38 DNA oligonucleotide forms a saturated filament with G5P up to a Nt/G5P ratio $n=4$. At Nt/G5P ratios below $n=4$ (high G5P concentrations) an excess of G5P exist. The Cy3 fluorescence increases with further addition of G5P due to PIFE effect (see below). Compared to this, for the oligonucleotide with Cy3 and BHQ2 quencher but no defined secondary

1
2
3 structure a decrease of the fluorescence persists down to about $n=1.5$. The fact that the
4 decrease in the Cy3 intensity in the case of the oligonucleotide incorporating both Cy3 and
5 the quencher proceeds up to $n=1.5$ could be related to changes of the relative orientation of
6 the Cy3 and the quencher dipole moment induced by G5P.³¹ At Nt/G5P ratios below $n=1.5$
7 an increase of the fluorescence signal can be detected (close up).
8
9

10
11 The photophysical properties of Cy3 have been well studied.³²⁻³⁴ There it was observed, that
12 after excitation, in addition to the radiative decay pathway generating fluorescence, Cy3 can
13 also isomerize from the trans- to the cis- configuration through a torsional motion, bringing
14 Cy3 back to its ground state without photon emission. Such a behaviour, when the close
15 proximity of a protein to Cy3 leads to enhancement of the fluorescence intensity, is the ba-
16 sis of Protein Induced Fluorescence Enhancement (PIFE).³⁵ PIFE is a versatile method for
17 studying protein-DNA interactions which uses a single fluorophore³⁶ and has sensitivity at
18 distances that are shorter than that of the FRET range.³⁷ PIFE occurs in environmentally
19 sensitive fluorophores of the cyanine dyes³⁸ and has been explained by a decrease in the rate
20 of the cis-trans photoisomerization^{35,38} due to protein influence on the rate of photoisomer-
21 ization through steric hindrance³⁹ and specific contact with specific amino acids residues of
22 the protein.^{35,38} In addition, influence of the solution viscosity on the fluorescence intensity
23 of Cy3 has been proposed.⁴⁰ Thus, the fluorescence intensity of free Cy3 in solution increased
24 more than fourfold as viscosity was varied about a factor of twenty by varying the concen-
25 tration of glycerol or ethanol in PBS.⁴⁰ However, the experimental condition in this study
26 support the explanation that proteins additionally bound closely to Cy3 in the ssDNA/G5P
27 complex are responsible for PIFE for the following reasons. We note here that in case of
28 BamHI protein system a twofold decrease in PIFE was observed already for distance changes
29 of only one base pair, which is less than 3.4 Å.³⁷ BamHI displays PIFE sensitivity in a range
30 of 10 base pairs.³⁷ On the other hand, for our experimental parameters (excitation at 532
31 nm and a 0.4 NA objective) the confocal volume is about 1 fL. A local concentration of 1 μM
32 of oligonucleotides corresponds to about 600 molecules in the confocal volume, and 38 μM of
33
34
35
36
37
38
39
40
41
42
43
44
45
46
47
48
49
50
51
52
53
54
55
56
57
58
59
60

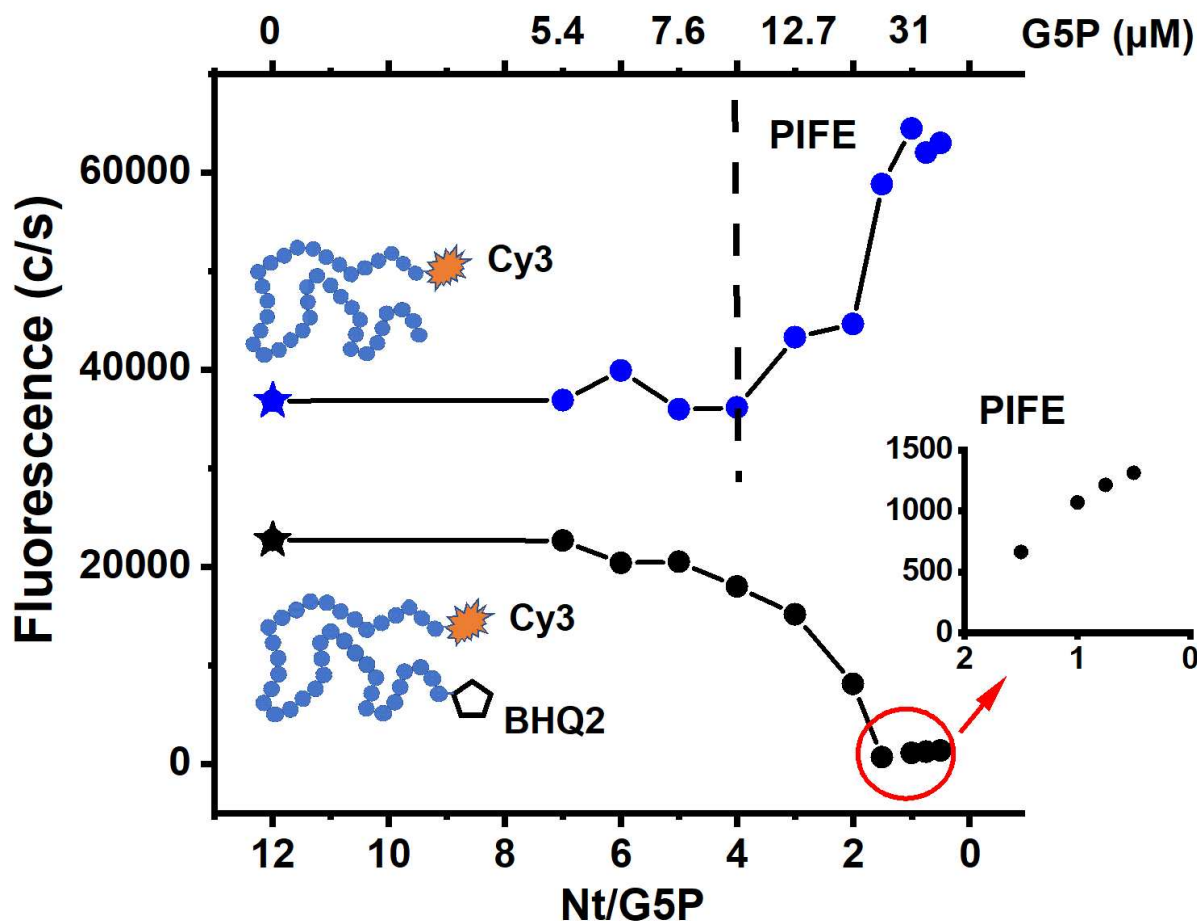


Figure 6: Comparison of the Cy3-fluorescence intensities of Cy3-dT38 (control oligonucleotide) and Cy3-dT38-BHQ2 oligonucleotides of the same length, as the function of the nucleotide/G5P ratio ($n=Nt/G5P$). The data were obtained within one experiment under identical experimental conditions. The oligonucleotide concentration after mixing with G5P was $1\mu\text{M}$ in both cases. The lowest and highest G5P concentrations after mixing with oligonucleotides are $5.43\mu\text{M}$ ($n=7$) and $76\mu\text{M}$ ($n=0.5$), respectively. The fluorescence intensities of the two oligonucleotides at $1\mu\text{M}$ concentration without G5P in the solution are indicated in the figure with stars positioned arbitrary at the end of the range at $n=12$. The PIFE effect sets in at different Nt/G5P ratios, depending on the absence or presence of the quencher.

1
2
3 G5P ($n=1$ for 38mer oligonucleotide) to about 23000 G5P molecules forming 11500 dimers
4
5 of approximately 48 nm^3 in the confocal volume. Even at this high protein concentration the
6
7 total volume of all proteins together is more than 1600-fold smaller than the confocal volume,
8
9 making viscosity effects unlikely cause of PIFE. Thus, a direct interaction of G5P bound to
10
11 ssDNA is, therefore, a likely cause here for following reasons. If one G5P dimer requires
12
13 4 bps to attach, Cy3-dT18stem7-(BHQ2) can bind up to 4 dimers and Cy3-dT38 up to 5
14
15 dimers until full saturation. At a ratio of $1 \text{ }\mu\text{M}$ oligos to $76 \text{ }\mu\text{M}$ G5P, consecutive binding of
16
17 G5P alone could be sufficient to induce PIFE in the presence/absence of the quencher. The
18
19 binding at low G5P concentration should not affect Cy3, which is, in particular, true when
20
21 the complex is not static and G5P can still slide along. For increasing G5P concentration,
22
23 more and more dimers will bind to the ssDNA forming a loop and then form a filament as
24
25 depicted in Fig. 8. In the quenching assay, this will bring Cy3 and BHQ2 together and lead to
26
27 a decrease in fluorescence. With increased binding, PIFE will occur in parallel (which is still
28
29 majorly quenched) but visible at higher concentrations. In the PIFE assay, this consecutive
30
31 binding will not be seen at the beginning, but only for $n < 4$ when more molecules are bound
32
33 until sufficient G5P molecules bind to the filament so that Cy3 starts being influenced by
34
35 the presence of G5P. This interpretation would be in line with MBs, where the additional
36
37 G5Ps start opening the beacon in addition (see below).

38
39 In Fig.7 (left) we present equilibrium fluorescence of the hairpin oligonucleotide loop18stem7
40
41 as a function of $n=Nt/G5P$. The protein binds first the loop and saturates it. At higher pro-
42
43 tein concentrations the protein starts to open the stem region (unwinding process). To
44
45 test the hypothesis that 2 complexes were formed at different $Nt/G5P$ ratios, we have per-
46
47 formed EMSA experiments (Fig.7, right), whose results are in good agreement with the step
48
49 wise formation of G5P/DNA complexes and fits to the proposed unzipping of the hairpin
50
51 structure as explained in the following. Thus, even though the G5P has been usually consid-
52
53 ered as a sequence independent ssDNA binding protein, the early data of Gray *et al.* have
54
55 identified DNA hairpins^{26,41} as being among the protein's preferred binding sites. The G5P-
56
57
58
59
60

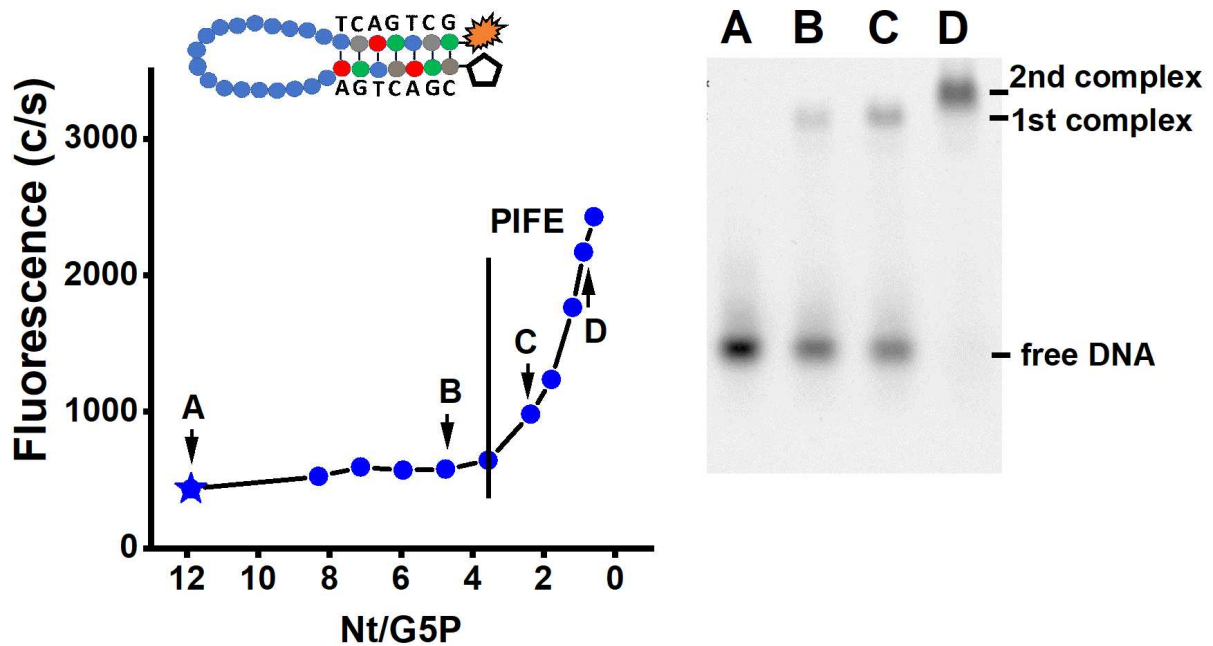


Figure 7: (Left) Cy3-fluorescence intensity of Cy3-dT18stem7-BHQ2 hairpin oligonucleotide as the function of the nucleotide/G5P ratio ($n=Nt/G5P$). Note that this ratio differs somewhat from the one in Fig.6 because the overall length of the hairpin oligonucleotide is 32 instead of 38. The oligonucleotide concentration after mixing with G5P was $1\mu M$. The lowest and highest G5P concentrations after mixing with the oligonucleotide are $5.43\mu M$ ($n=8.31$) and $76\mu M$ ($n=0.59$), respectively. The fluorescence intensities of the oligonucleotide at $1\mu M$ concentration without G5P in the solution is indicated in the figure with a star positioned arbitrary at the end of the range at $n=12$. The protein binds first the loop. At higher protein concentrations the protein starts to open the stem region (unwinding process). The formation of such a filamentous complex results in the 2nd complex observed in the EMSA. The PIFE effect is observed at $n>4$. (Right) Electrophoretic mobility shift assay (EMSA) of $2.5\mu M$ dT18stem7 hairpin oligonucleotide and different G5P concentrations: A) no protein, B) $17.5\mu M$, C) $35\mu M$, and D) $75\mu M$. The proposed binding scenarios are marked in the figure.

1
2
3 binding affinity to hairpins was estimated to be about 40-fold higher compared to ssDNA
4 without hairpins. Their EMSA experiments show a two step binding of G5P to the hairpin
5 structure.^{26,41} Considering this, and the fact that G5P has dyadic DNA-binding sites, we
6 conclude that G5P first binds to the loop region of the hairpin (Fig.7 right, Lane B and C),
7 and in a second step the stem region is opened and the whole DNA covered with G5P (Fig.7
8 right, Lane D).²⁶ It is important to note here that these data are obtained by imaging the
9 Cy3-fluorescence directly, and not as usual by a posterior staining of the gel. Therefore free
10 G5P is not detected in this experiment, but only free ssDNA and the ssDNA-G5P complex.
11 The initial intermediate complex is found to be a stable complex, in the sense that it does
12 not facilitate the binding of further G5P dimers to the stem. However, the unzipping of
13 the stem, and the formation of a fully saturated complex can be initiated when the G5P
14 concentration is further increased above a critical point.²⁶

15
16
17 In Fig. 8 changes in the fluorescence intensity of two DNA probes upon two successive in-
18 jections are presented. These dynamic fluorescence data compare two oligonucleotide probes,
19 one with (blue curve) and the other without (red curve) hairpin structure. The data was
20 obtained using a microfluidics mixer (Fig.3) as described in the experimental section. In the
21 case of the oligonucleotide without hairpin structure (red curve) injection and mixing with
22 G5P results in a sharp peak during injection and an extended region of very low intensity.
23 This is in accordance with the known fast sequestering of ssDNA by G5P and merging of
24 the ssDNA ends with Cy3 and BHQ2, bringing them in proximity. In contrast, the hairpin
25 oligonucleotide (blue curve) with double-stranded stem shows a prominent broad peak. We
26 tentatively assign this broad peak, which stretches over few tens of seconds, to processes
27 involved in unzipping of the stem and the formation of the fully saturated complex. In this
28 scenario, the stem⁷ is destabilized, most likely from the loop-side of the oligonucleotide,
29 as G5P interacts with a few nucleotides of the stem. The shorter rest of the stem is then
30 becoming destabilized, leading to a higher rate of opening and therefore to an increase in
31 fluorescence intensity. At the same time, an unzipped stem is an appropriate conformation
32
33
34
35
36
37
38
39
40
41
42
43
44
45
46
47
48
49
50
51
52
53
54
55
56
57
58
59
60

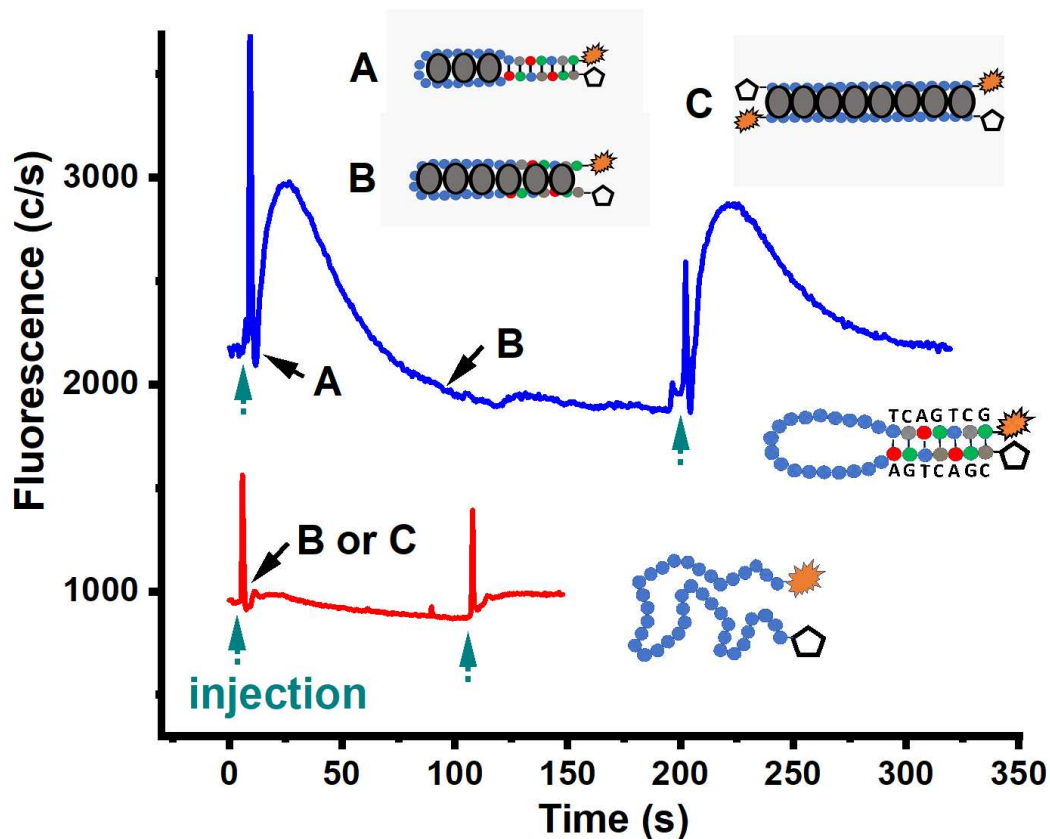


Figure 8: Cy3 fluorescence upon mixing of two DNA oligonucleotide and G5P using a microfluidics mixer. The curves show two successive experiments (mixing) using a hairpin DNA (blue curve above, dT38stem7) and a ssDNA without a secondary structure (red curve below, dT38). The DNA and G5P concentrations are $0.5 \mu\text{M}$ and $5 \mu\text{M}$, respectively. Structure A corresponds to the structure where G5P has bound only to the hairpin region, while structure B depicts a fully saturated nucleoprotein filament. Structure C corresponds to two antiparallel bound ssDNA strands involving two dT38stem7 oligonucleotides. This structure is generally considered less likely in the case of equilibrium measurements, but is proposed here because the microfluidic data concern flow and high pressure conditions. However, with the experimental set-up we can not discriminate between structure B and C. Mixing dT38stem7 with G5P results in a broad fluorescence peak stretching over about 50 seconds. During this time, the unzipping of the stem starts increasing fluorescence. In parallel complexes B and C are formed decreasing fluorescence. The two processes result in the fluorescence peak. For the sequence dT38 (no DNA hairpin) time dependent changes of the fluorescence can not be detected as the saturated complex is formed within ms range. The fluorograms are shifted vertically for clarity.

1
2
3 for further binding of G5P and therefore for reduction of the fluorescence intensity. These
4 two competing processes happening in the ensemble of molecules measured lead to the broad
5 peak observed in Fig.8. This finding and proposed model is consistent with the two-stage
6 binding of G5P to hairpins observed in Fig.7 (right) and early EMSA studies,²⁶ concerning
7 the G5P-hairpin interaction. We note here that other single-stranded DNA-binding proteins
8 also destabilize secondary DNA structures such as hairpins. Thus, using single molecule total
9 internal reflection fluorescence microscopy, a fluctuating smFRET signal is observed, which
10 is consistent with the unzipping of the hairpin by SSB protein in two stages.^{6,7} In addition,
11 using a single-molecule fluorescence approach, Nguyen *et al.*⁸ showed that human Replica-
12 tion Protein A (hRPA) protein diffuses along ssDNA to transiently invade and destabilize
13 (unzip) a DNA hairpin structure. In conclusion, we propose that in the case of the hairpin
14 oligonucleotides used in this study, an intermediate complex (where G5P binds antiparallel
15 strands in the loop region) is immediately formed upon mixing with the protein. This is
16 followed by a destabilization of the stem, as observed by the broad and delayed fluorescence
17 feature after mixing, until the fully saturated DNA-protein complex is formed.
18
19
20
21
22
23
24
25
26
27
28
29
30
31
32

33 The molecular beacon data presented in this work are the first results applying a fluoro-
34 metric approach concerning the interaction of G5P with DNA and represent a base for the
35 future investigations with methods such as smFRET.⁴² Finally, it is important to note here,
36 that the described results should be largely considered as model studies of importance in
37 (bio)nanotechnology and spectroscopy.
38
39
40
41
42
43
44

45 Acknowledgement

46
47
48 The authors thank Heinz Sturm for valuable discussions. This work was funded by the
49 Deutsche Forschungsgemeinschaft (DFG, German Research Foundation) under grant number
50 442240902 (HA 8528/2-1 and SE 2999/2-1).
51
52
53
54
55
56
57
58
59
60

References

- (1) Lohman, T. M.; Ferrari, M. E. Escherichia Coli Single-Stranded DNA-binding Protein: Multiple DNA-binding Modes and Cooperativities. *Annu Rev Biochem* **1994**, *63*, 527–570.
- (2) Meyer, R. R.; Laine, P. S. The Single-Stranded DNA-binding Protein of Escherichia Coli. *Microbiol Rev* **1990**, *54*, 342–380.
- (3) Roy, R.; Kozlov, A. G.; Lohman, T. M.; Ha, T. Dynamic Structural Rearrangements Between DNA Binding Modes of E. Coli SSB Protein. *Journal of Molecular Biology* **2007**, *369*, 1244–1257.
- (4) Muniyappa, K.; Shaner, S. L.; Tsang, S. S.; Radding, C. M. Mechanism of the Concerted Action of recA Protein and Helix-Destabilizing Proteins in Homologous Recombination. *Proceedings of the National Academy of Sciences* **1984**, *81*, 2757–2761.
- (5) Eggington, J. M.; Kozlov, A. G.; Cox, M. M.; Lohman, T. M. Polar Destabilization of DNA Duplexes with Single-Stranded Overhangs by the Deinococcus Radiodurans SSB Protein. *Biochemistry* **2006**, *45*, 14490–14502.
- (6) Roy, R.; Kozlov, A. G.; Lohman, T. M.; Ha, T. SSB Protein Diffusion on Single-Stranded DNA Stimulates RecA Filament Formation. *Nature* **2009**, *461*, 1092–1097.
- (7) Sokoloski, J. E.; Kozlov, A. G.; Galletto, R.; Lohman, T. M. Chemo-Mechanical Pushing of Proteins along Single-Stranded DNA. *Proceedings of the National Academy of Sciences* **2016**, *113*, 6194–6199.
- (8) Nguyen, B.; Sokoloski, J.; Galletto, R.; Elson, E. L.; Wold, M. S.; Lohman, T. M. Diffusion of Human Replication Protein A along Single-Stranded DNA. *Journal of Molecular Biology* **2014**, *426*, 3246–3261.

- 1
2
3
4 (9) Li, J.; Cao, Z. C.; Tang, Z.; Wang, K.; Tan, W. In *Molecular Beacons: Signalling*
5 *Nucleic Acid Probes, Methods, and Protocols*; Marx, A., Seitz, O., Eds.; Methods in
6 Molecular Biology; Humana Press: Totowa, NJ, 2008; pp 209–224.
7
8
9
10 (10) Olah, G. A.; Gray, D. M.; Gray, C. W.; Kergil, D. L.; Sosnick, T. R.; Mark, B. L.;
11 Vaughan, M. R.; Trehwella, J. Structures of Fd Gene 5 Protein·Nucleic Acid Complexes:
12 A Combined Solution Scattering and Electron Microscopy Study. *Journal of Molecular*
13 *Biology* **1995**, *249*, 576–594.
14
15
16
17
18 (11) Scheerhagen, M. A.; Bokma, J. T.; Vlaanderen, C. A.; Blok, Joh.; Van Grondelle, R.
19 A Specific Model for the Conformation of Single-Stranded Polynucleotides in Complex
20 with the Helix-Destabilizing Protein GP32 of Bacteriophage T4. *Biopolymers* **1986**,
21 *25*, 1419–1448.
22
23
24
25
26
27 (12) Solomun, T.; Sturm, H.; Wellhausen, R.; Seitz, H. Interaction of a Single-Stranded
28 DNA-binding Protein G5p with DNA Oligonucleotides Immobilised on a Gold Surface.
29 *Chemical Physics Letters* **2012**, *533*, 92–94.
30
31
32
33
34 (13) Hahn, M. B.; Solomun, T.; Wellhausen, R.; Hermann, S.; Seitz, H.; Meyer, S.;
35 Kunte, H.-J.; Zeman, J.; Uhlig, F.; Smiatek, J. et al. Influence of the Compatible Solute
36 Ectoine on the Local Water Structure: Implications for the Binding of the Protein G5P
37 to DNA. *J. Phys. Chem. B* **2015**, *119*, 15212–15220.
38
39
40
41
42
43 (14) Hallier, D. C.; Smales, G. J.; Seitz, H.; Hahn, M. B. Bio-SAXS of Single-Stranded
44 DNA-binding Proteins: Radiation Protection by the Compatible Solute Ectoine. *Phys.*
45 *Chem. Chem. Phys.* **2023**, *25*, 5372–5382.
46
47
48
49
50 (15) Shamir, Y.; Goldbourt, A. Atomic-Resolution Structure of the Protein Encoded by
51 Gene V of Fd Bacteriophage in Complex with Viral ssDNA Determined by Magic-
52 Angle Spinning Solid-State NMR. *J. Am. Chem. Soc.* **2023**, *145*, 300–310.
53
54
55
56
57
58
59
60

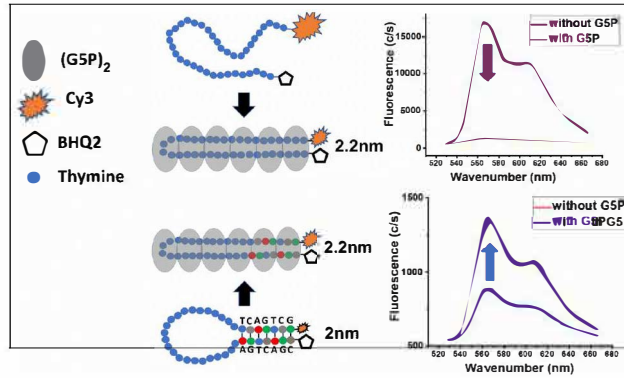
- 1
2
3
4 (16) Cheng, X.; Harms, A. C.; Goudreau, P. N.; Terwilliger, T. C.; Smith, R. D. Direct
5 Measurement of Oligonucleotide Binding Stoichiometry of Gene V Protein by Mass
6 Spectrometry. *Proceedings of the National Academy of Sciences* **1996**, *93*, 7022–7027.
7
8
9
10 (17) Hahn, M. B.; Dietrich, P. M.; Radnik, J. In Situ Monitoring of the Influence of Water on
11 DNA Radiation Damage by Near-Ambient Pressure X-ray Photoelectron Spectroscopy.
12 *Commun Chem* **2021**, *4*, 50.
13
14
15 (18) Hahn, M. B. Accessing Radiation Damage to Biomolecules on the Nanoscale by Particle-
16 Scattering Simulations. *J. Phys. Commun.* **2023**, *7*, 042001.
17
18
19 (19) Skinner, M. M.; Zhang, H.; Leschnitzer, D. H.; Guan, Y.; Bellamy, H.; Sweet, R. M.;
20 Gray, C. W.; Konings, R. N.; Wang, A. H.; Terwilliger, T. C. Structure of the Gene V
21 Protein of Bacteriophage F1 Determined by Multiwavelength X-Ray Diffraction on the
22 Selenomethionyl Protein. *PNAS* **1994**, *91*, 2071–2075.
23
24
25 (20) Murzin, A. G. OB(Oligonucleotide/Oligosaccharide Binding)-fold: Common Structural
26 and Functional Solution for Non-homologous Sequences. *The EMBO Journal* **1993**, *12*,
27 861–867.
28
29
30 (21) Su, S.; Gao, Y.-G.; Zhang, H.; Terwilliger, T. C.; Wang, A. H.-J. Analyses of the
31 Stability and Function of Three Surface Mutants (R82C, K69H, and L32R) of the
32 Gene V Protein from Fφ Phage by X-ray Crystallography. *Protein Science* **1997**, *6*,
33 771–780.
34
35
36 (22) Terwilliger, T. C. Gene V Protein Dimerization and Cooperativity of Binding to Poly
37 (dA). *Biochemistry* **1996**, *35*, 16652–16664.
38
39
40 (23) Bulsink, H.; Harmsen, B. J.; Hilbers, C. W. Specificity of the Binding of Bacteriophage
41 M13 Encoded Gene-5 Protein to DNA and RNA Studied by Means of Fluorescence
42 Titrations. *Journal of Biomolecular Structure and Dynamics* **1985**, *3*, 227–247.
43
44
45
46
47
48
49
50
51
52
53
54
55
56
57
58
59
60

- 1
2
3
4 (24) Kansy, J. W.; Clack, B. A.; Gray, D. M. The Binding of Fd Gene 5 Protein to Poly-
5 deoxynucleotides: Evidence from CD Measurements for Two Binding Modes. *Journal*
6 *of Biomolecular Structure and Dynamics* **1986**, *3*, 1079–1110.
7
8
9
10 (25) Thompson, T. M.; Mark, B. L.; Gray, C. W.; Terwilliger, T. C.; Sreerama, N.;
11 Woody, R. W.; Gray, D. M. Circular Dichroism and Electron Microscopy of a Core
12 Y61F Mutant of the F1 Gene 5 Single-Stranded DNA-Binding Protein and Theoret-
13 ical Analysis of CD Spectra of Four Tyr Phe Substitutions. *Biochemistry* **1998**, *37*,
14 7463–7477.
15
16
17
18
19
20 (26) Wen, J.-D.; Gray, D. M. Ff Gene 5 Single-Stranded DNA-binding Protein Assembles
21 on Nucleotides Constrained by a DNA Hairpin. *Biochemistry* **2004**, *43*, 2622–2634.
22
23
24
25 (27) Gray, C. W. Three-Dimensional Structure of Complexes of Single-Stranded DNA-
26 binding Proteins with DNA: IKE and Fd Gene 5 Proteins Form Left-Handed Helices
27 with Single-Stranded DNA. *Journal of Molecular Biology* **1989**, *208*, 57–64.
28
29
30
31 (28) Solomun, T.; Hahn, M. B.; Smiatek, J. Raman Spectroscopic Signature of Ectoine
32 Conformations in Bulk Solution and Crystalline State. *ChemPhysChem* **2020**, *21*, 1945–
33 1950.
34
35
36
37
38 (29) Murphy, M. C.; Rasnik, I.; Cheng, W.; Lohman, T. M.; Ha, T. Probing Single-Stranded
39 DNA Conformational Flexibility Using Fluorescence Spectroscopy. *Biophysical Journal*
40 **2004**, *86*, 2530–2537.
41
42
43
44 (30) Kuznetsov, S. V.; Ren, C.-C.; Woodson, S. A.; Ansari, A. Loop Dependence of the
45 Stability and Dynamics of Nucleic Acid Hairpins. *Nucleic Acids Research* **2008**, *36*,
46 1098–1112.
47
48
49
50
51 (31) Förster, T. *Modern Quantum Chemistry*; O. Sinanoglu (Ed.); Academic Press: New
52 York and London, 1965; Vol. Istanbul Lectures. Part III: Action of Light and Organic
53 Crystals; pp 93–137.
54
55
56
57
58
59
60

- 1
2
3
4 (32) Aramendia, P. F.; Negri, R. M.; Roman, E. S. Temperature Dependence of Fluorescence
5 and Photoisomerization in Symmetric Carbocyanines. Influence of Medium Viscosity
6 and Molecular Structure. *J. Phys. Chem.* **1994**, *98*, 3165–3173.
7
8
9
10 (33) Levitus, M.; Ranjit, S. Cyanine Dyes in Biophysical Research: The Photophysics of
11 Polymethine Fluorescent Dyes in Biomolecular Environments. *Quarterly Reviews of*
12 *Biophysics* **2011**, *44*, 123–151.
13
14
15
16 (34) Muddana, H. S.; Morgan, T. T.; Adair, J. H.; Butler, P. J. Photophysics of Cy3-
17 Encapsulated Calcium Phosphate Nanoparticles. *Nano Lett.* **2009**, *9*, 1559–1566.
18
19
20
21 (35) Stennett, E. M. S.; Ciuba, M. A.; Lin, S.; Levitus, M. Demystifying PIFE: The Photo-
22 physics Behind the Protein-Induced Fluorescence Enhancement Phenomenon in Cy3.
23 *J. Phys. Chem. Lett.* **2015**, *6*, 1819–1823.
24
25
26
27
28 (36) Hwang, H.; Myong, S. Protein Induced Fluorescence Enhancement (PIFE) for Probing
29 Protein–Nucleic Acid Interactions. *Chemical Society Reviews* **2014**, *43*, 1221–1229.
30
31
32
33 (37) Hwang, H.; Kim, H.; Myong, S. Protein Induced Fluorescence Enhancement as a Single
34 Molecule Assay with Short Distance Sensitivity. *Proceedings of the National Academy*
35 *of Sciences* **2011**, *108*, 7414–7418.
36
37
38
39
40 (38) Ploetz, E.; Lerner, E.; Husada, F.; Roelfs, M.; Chung, S.; Hohlbein, J.; Weiss, S.;
41 Cordes, T. Förster Resonance Energy Transfer and Protein-Induced Fluorescence En-
42 hancement as Synergetic Multi-Scale Molecular Rulers. *Sci Rep* **2016**, *6*, 33257.
43
44
45
46
47 (39) Gatzogiannis, E.; Chen, Z.; Wei, L.; Wombacher, R.; Kao, Y.-T.; Yefremov, G.; W. Cor-
48 nish, V.; Min, W. Mapping Protein -Specific Micro-Environments in Live Cells by
49 Fluorescence Lifetime Imaging of a Hybrid Genetic-Chemical Molecular Rotor Tag.
50 *Chemical Communications* **2012**, *48*, 8694–8696.
51
52
53
54
55
56
57
58
59
60

- 1
2
3
4 (40) Luby-Phelps, K.; Mujumdar, S.; Mujumdar, R. B.; Ernst, L. A.; Galbraith, W.; Wag-
5 goner, A. S. A Novel Fluorescence Ratiometric Method Confirms the Low Solvent Vis-
6 cosity of the Cytoplasm. *Biophysical Journal* **1993**, *65*, 236–242.
7
8
9
10 (41) Wen, J.-D.; Gray, C. W.; Gray, D. M. SELEX Selection of High-Affinity Oligonu-
11 cleotides for Bacteriophage Ff Gene 5 Protein. *Biochemistry* **2001**, *40*, 9300–9310.
12
13
14
15 (42) Roy, R.; Hohng, S.; Ha, T. A Practical Guide to Single-Molecule FRET. *Nature methods*
16 **2008**, *5*, 507–516.
17
18
19
20
21
22
23
24
25
26
27
28
29
30
31
32
33
34
35
36
37
38
39
40
41
42
43
44
45
46
47
48
49
50
51
52
53
54
55
56
57
58
59
60

TOC Graphic



The interaction of a dimeric single-stranded DNA-binding protein (G5P) with DNA molecular beacons.